RSC Advances

This is an *Accepted Manuscript*, which has been through the Royal Society of Chemistry peer review process and has been accepted for publication.

Accepted Manuscripts are published online shortly after acceptance, before technical editing, formatting and proof reading. Using this free service, authors can make their results available to the community, in citable form, before we publish the edited article. This *Accepted Manuscript* will be replaced by the edited, formatted and paginated article as soon as this is available.

You can find more information about *Accepted Manuscripts* in the Information for Authors.

Please note that technical editing may introduce minor changes to the text and/or graphics, which may alter content. The journal's standard Terms & Conditions and the Ethical guidelines still apply. In no event shall the Royal Society of Chemistry be held responsible for any errors or omissions in this *Accepted Manuscript* or any consequences arising from the use of any information it contains.

ROYAL SOCIETY OF CHEMISTRY

www.rsc.org/advances

Title of the paper: **Development and complex characterization of bio- tribological Cr/CrN + a-C:H (dopped Cr) nano- multilayer protective coatings for carbon- fiber- composite materials**

L. Major[1], M. Janusz[1], M. Kot[2], J.M. Lackner[3], B. Major[1]

[1] Institute of Metallurgy and Materials Science; Polish Academy of Sciences, 30-059 Cracow, 25 Reymonta Street, Cracow, Poland

[2] AGH University of Science and Technology, Faculty of Mechanical Engineering and Robotics, Laboratory of Surface Engineering and Tribology, Al. Mickiewicza 30, PL-30059 Cracow, Poland

[3] JOANNEUM RESEARCH- Materials- Institute for Surface Technologies and Photonics; Leobner Strasse 94; 8712 Niklasdorf, Austria

Corresponding author : Lukasz Major

Full Mailing Address : Institute of Metallurgy and Materials Science Polish Academy of Sciences; 25 Reymonta Street; 30-059 Cracow; Poland

Telephone : +48-12-2952800

Fax : +48-12-2952804

E-mail : l.major@imim.pl

RSC Advances Accepted Manuscript

Development and complex characterization of bio- tribological Cr/CrN + a-C:H (dopped Cr) nano- multilayer protective coatings for carbon- fiber- composite materials

L. Major[1], M. Janusz[1], M. Kot[2], J.M. Lackner[3], B. Major[1]

[1] Institute of Metallurgy and Materials Science; Polish Academy of Sciences, 30-059 Cracow, 25 Reymonta Street, Cracow, Poland

[2] AGH University of Science and Technology, Faculty of Mechanical Engineering and Robotics, Laboratory of Surface Engineering and Tribology, Al. Mickiewicza 30, PL-30059 Cracow, Poland

[3] JOANNEUM RESEARCH- Materials- Institute for Surface Technologies and Photonics; Leobner Strasse 94; 8712 Niklasdorf, Austria

Contents entry

Novel aspects are innovative, protective, coatings for carbon- fiber- composite materials elaboration, unique and advanced techniques of the coatings deposition and complex characterization of their microstructure and bio- tribological properties .

Abstract

Carbon fiber structures provide strength, stiffness, and fatigue resistance. Carbon-based materials show, however, significant oxidative degradation in air beginning at temperatures in the region of 400 degree C. Therefore, a coating concept for carbon–carbon composites

RSC Advances Accepted Manuscript

consist of an inner part, which serves as structural link with stress compensation ability to the carbon substrate, and an outer part, which acts as a diffusion barrier. In the presented paper, as the inner part chromium/ chromium nitride (Cr/CrN) multilayer structure has been selected. The outer part of the coating, in the presented paper, was hydrogenated amorphous carbon (a-C:H). Among doping metals, Cr as one of carbide formed elements possesses an attractive combination of properties (corrosion resistance, wear resistance, etc.). Thus, in the presented paper a-C:H part of the coating was implanted by Cr nanocrystals. Coatings were deposited by means of magnetron sputtering technique. They were subjected to complex investigations. Mechanisms of a mechanical wear of analyzed systems were presented, focusing on the cracking propagation in ball- on- disc tests using a 1N and 5 N applied loads for 20000 cycles. Complex microstructure analysis of presented, nano- multilayer coatings, before and after mechanical tests, were performed by means of transmission electron microscopy (TEM). The microstructure characterization revealed that cracking which was propagating in the outer part of the coating (in the carbon part) in the layer with lower nano- particle content was stopped at the interface with the higher nano- particle content layer. In case of inner part of the coating (Cr/Cr_2N), ceramic layers brittle cracked, while metallic (Cr) ones plastically deformed.

Keywords: Nano- multilayer coating, Carbon- Fiber- Composite, Microstructure,
Bio- Tribology

1. Introduction

Carbon- carbon (C/C) composite or Carbon- Fiber- Composite (CFC) are increasingly being considered for aerospace application. In composite materials, the fibers impart strength, stiffness and fatigue resistance, while the carbon matrix holds the fibers together.

RSC Advances Accepted Manuscript

A synergistic effect also exists between the fiber and the carbon matrix which results in high fracture toughness and wear resistance. But the most attractive properties of carbon- fiber-composites are their high specific strength and modulus. Based on their good mechanical performances, potential uses of structural carbon materials have been identified in future manned hypersonic vehicles and in other aircraft applications. However, most of these applications involve extended time periods in oxidizing environments. Unfortunately, carbon reacts rapidly with oxygen at temperatures round 500°C and the composites are subject to oxidation degradation. Less is known about the effect of oxidation on the properties of CFC, because they vary with the oxidation mechanisms and micro- structural features of the materials. But it is well known that oxidation degrades quickly the properties of carbon materials. Therefore, numerous investigations have been conducted in an attempt to protect carbon based composites against oxidation.[1] Two ways are commonly used for the oxidation protection of CFC. The first one consist in the addition of some oxidation inhibitors into the matrix of the composite (such as phosphorous-, boron-, or silicon-containing additives).[2] These additives can effectively lower the oxidation rate of the CFC but they are not efficient for prolonged time at temperatures above 900- 1000°C. The second way is the deposition of external coatings on the composite surface, however, the biggest problem is thermal expansion mismatch between the coating material and the carbon substrates. Some attempts have been proposed in this field.[3-6]

Applicable coating techniques are electrochemical/galvanic deposition or thermal and plasma spraying, which provide thick coatings of high load support.[7-9] However, they lack in adhesion during overloading, since their stiffness is too high and their plastic deformability is too low to follow substrate deflection. Alternatively, thick soft polymer coatings (pure and micro-/nanoparticle strengthened lacquers) possess high elasticity for bending to follow substrate deflection, but they fail in tribological resistance.[10] Thin films of materials

RSC Advances Accepted Manuscript

combining hardness and wear resistance with high compliance as well as high resistance to cohesive and adhesive crack propagation (high toughness) are future candidates for surface protection of high performance polymers.[11-13] Kääriäinen et al. proposed chromium nitride (CrNx) single layer coatings on CFC, but they were not effective in tribological protection.[14] Although they achieved high adhesion of the magnetron-sputtered PVD coatings due to surface activation by high ion doses before film deposition or high substrate temperature, the realization of dense coatings was impossible. This was assigned to a very inhomogeneous and rough substrate surface, consisting of fibers with loose ends and polymer filler.

The paper deals with the modern coatings development with appropriate adhesion to CFC substrate. In case of coatings for carbon composite substrates, the proper coatings materials selection is essential. Currently, in surface modification much attention is directed to multilayer coatings. The set of alternate layers of hard and soft phases as well as appropriate buffer layer application (the first layer from the substrate) can lead to coating quality improvement and the increase of adhesion to the substrate.[15-19] In case of protective coatings for CFC the quality and type of first buffer layer is the most essential, due to the differences in thermal expansion coefficient and possibilities of high residual stress formation especially at the coating/ substrate interface. Multilayer coatings are composed of alternately stacked layers of hard and soft phases with thicknesses of a few to tens of nanometers. This combination of alternate layers may lead to considerable hardness, and high flexibility, good adhesion coatings to substrates as well as may lead to self- healing effect, what is important in substrate protection against oxidation. Possible cracks propagation through ceramic coating can be stopped at the ceramic/metallic interface by plastic flow. Energy of brittle cracking is compensate by plastic deformation. coating concept for carbon–carbon

RSC Advances Accepted Manuscript

composites should consist of an inner part, which serves as structural link with stress compensation ability to the carbon substrate, and an outer part, which acts as a diffusion barrier. In the presented paper, as the inner part chromium/ chromium nitride (Cr/CrN) multilayer structure has been selected. The literature data indicates the particular meaning of Cr and CrN multilayer coatings. They are characterized by an appropriate crystallographic adjustment of subsequent constituent layers of Cr and CrN and by the creation of a transition layer between them with a thickness of several dozen of nanometers. This ensures a good connection between particular constituent layers and as a result also good maintenance properties: high adhesion, wear and corrosive resistance.[20] The outer part of the coating, in the presented paper, was hydrogenated amorphous carbon (a-C:H). It is well-known that a-C:H coatings have low- friction coefficients and low-specific wear rates. Thus, the amorphous carbon coatings are very promising tribo- materials. However, the poor adhesion strength to substrate, high residual stress and weak thermal stability would limit their application. Currently, many metallic elements (Ti, W, Ag, Cr etc.) have been utilized to modify their structure, and it has been proved that the metal doping is an effective method to reduce residual stress and enhance adhesion strength of the film.[21] In the presented paper a-C:H part of the coating was implanted by Cr nanocrystals. The presented paper deals with microstructure description of the as deposited coatings as well as with microstructure changes description of the coatings after mechanical wear. The elaborated materials are designed de novo for the elements of surgical tools. Thus the coatings should be assembled to express biocompatible properties and not being recognized by human enzymatic degradation system as well as they should be characterized by adequate mechanical properties namely be wear resistant.

RSC Advances Accepted Manuscript

2. Materials and Methods

2.1. Deposition technique

A hybrid PLD system (Pulsed Laser Deposition + magnetron sputtering) equipped with a high purity chromium (99.9% Cr) and carbon (graphite) targets were used for multilayer coatings deposition. The described coating contained two parts. Cr/Cr_xN (chromium/ chromium nitride) multilayer was deposited as a inner part, first from CFC substrate. The outer part was amorphous carbon (a-C:H) gradually implanted by chromium nano- crystals. Details of the deposition process had been described elsewhere.[22] Coatings were deposited in four different deposition parameters set, as it is presented in the table (Table 1). "A" variant and "B" variant differed only in deposition conditions. One third of the carbon part of the coating deposited in "A" variant was produced using 155 DC (Direct Current), while last two third in 230 DC. Two third of the carbon part of the coating deposited in "B" variant was produced using 155 DC, while last one third in 230 DC.

2.2. Mechanical experiments

The mechanical properties result from the proper microstructure design. The mechanical properties of the coatings were investigated by means of nano- indentation (Berkovich indenter) and a ball-on-disc mechanical test using a 1N and 5N applied loads for 20000 cycles. All mechanical tests were performed in natural atmosphere (in air). The Al_2O_3 alumina ball with 6mm diameter was used for the test. The linear speed of the ball which was applied in the test was 0.06 m/s. The both tests parameters are presented below:

a). Low stress condition:

Load FN=1N; Ball radius R=3mm; Cycle number n= 20.000; Friction radius r=5mm,

Linear speed v=0,06m/s;σ_H=0,45GPa

RSC Advances Accepted Manuscript

b). High stress condition:

Load FN=5N; Ball radius R=3mm; Cycle number n= 5.000; Friction radius r=4mm,

Linear speed v=0,05m/s; σ_H=0,8 GPa

The parameters of the test which were used in the test were the optimal one for this kind of coatings deposited on such type of substrate. Before each test performance the optimum test properties are usually look for. Each type of coating composition and substrate type require new parameters test.

2.3. Techniques of microstructure investigation

The microstructure of the as- deposited coatings and after the mechanical tests, was studied using transmission (TEM) (TECNAI G2 F20 FEG (200 kV)) electron microscope, which allows microstructure observation at the smallest scale.

Microstructure of all investigated coatings was similar. The difference in between coatings was only in deposition conditions. It has been decided to present microstructure of coating, which according to mechanical test results, was characterized by the best properties (Variant "A").

Observations were carried out using TEM bright field mode (TEM BF), scanning TEM mode (STEM- observations in contrast dependents from the atomic number Z) and especially the high resolution mode (HRTEM). Phase analysis were done using selected area electron diffraction technique (SAEDF) and HRTEM. Chemical composition was characterized by energy dispersive X-ray spectroscopy technique (EDS). Thin foils for TEM observations were prepared using focused ion beam technique (FIB), using gallium ions. Only this technique allows to prepare thin foils directly from the place of interest (in this case from wear tracks). The QUANTA 200 3D DualBeam was used for thin foils preparation.

RSC Advances Accepted Manuscript

2.4. Cytotoxic analysis

Microstructure should influence on the induction of inflammatory reactions that can start a rejection reaction or, in case of medical tools, complications in the surgery. Biological test were performed as a screening tool for potential application for medical tools.

The cytotoxic effect was determined according to the ISO 10993-5:2009 standards.[23] Samples in size of 1.5 cm^2 were placed in confluent mouse fibroblast (L929; ATCC) cultures (about 5 x 105 cells) and have been incubated for 48 hours at 37 ^oC. Then cells were stained by propidium iodide (PI). Cultures incubated either with the samples were analyzed in comparison with control cultures. Images were taken with the Exciter 5 confocal microscope equipped with a camera and quantified using AxioVision 4.8 software (Carl Zeiss MicroImaging). A statistical analysis (two-way ANOVA and Tukey post hoc test, P value smaller than 0.05 was considered as significant – Statistica 10.0 PL) was performed on three replicates from each treatment. The analysis revealed changes dependent on applied deposition parameter. The applied fluorescent marker (PI) is a colorant dye of the nuclei. It cannot penetrate the cell membrane to a continuous living cells. Therefore, a dead cells are stained. It penetrates into the interior of dead cells through damaged in the process of necrosis cell membranes and intercalates with DNA helix, emitting red light fluorescence (excitation 535 nm, emission 617 nm).

3. Results and Discussion

3.1. Microstructure characterization of the as deposited Cr/Cr_xN + a-C:H+ Cr nano multilayer coating deposited on Carbon Fiber Composite material.

Structure, microstructure, and nanostructure of surface treatments are critical aspects for surface engineering.[24]

RSC Advances Accepted Manuscript

Microstructure characterization of the as deposited protective multilayer coating, described in the presented paper, was mainly characterized using the transmission electron microscopy technique (TEM).

Thin foils for TEM observation have been cut using focused ion beam technique (FIB) perpendicular to the carbon fibers, what is well seen at the image obtained by scanning electron microscope (Fig. 1a). Looking at the cross- section in STEM mode (scanning transmission electron microscopy), the quality of the deposited coating on such complicated structure was very high (Fig. 1b). No delamination was noticed. The coating clearly reflects the surface roughness of the carbon- fiber- composite (CFC) substrate.

The described coating contained two parts. Cr/Cr_xN (chromium/ chromium nitride) multilayer was deposited as a first part from CFC substrate (inner part). The second part was amorphous carbon (a-C:H) gradually implanted by chromium nano- crystals (outer part) (Fig. 2).

The purpose of Cr/Cr_xN part was to reduce residual stress of total coating, especially at the substrate/ coating interface, as well as to enhance coating adhesion to CFC substrate.

Because of presence of a metallic phase (chromium- Cr), total coating had partially plastic properties. Such behavior has been described by the authors in their previous papers.[15-17] as well as by other researchers.[25] The CrN and Cr lattice parameters, allow a cube- on- cube close to epitaxial growth with a low mismatch (1.6%) (Fig. 3).[20] In the presented case, the same diffraction contrast went through interfaces. It confirmed crystallographic dependence in between Cr and Cr_xN phases. It is well seen on the TEM BF image (Fig. 2a).

High resolution analysis of the TEM technique (HRTEM), allowed to established the mismatch in between Cr and Cr_xN. It has been confirmed that the mismatch was at the level of 2.4Å. Even such good lattice fit caused formation of defects in the form of mixed dislocations in the structure of metallic phase (Cr) (Fig. 4). It has been also confirmed that Cr_xN was presented as a Cr_2N.

RSC Advances Accepted Manuscript

The presence of defects in the form of dislocations, can affect the strengthening of the structure of the metallic phase, which can impact positively on the mechanical properties of the whole coating.[18]

The second part of the coating, as it was mentioned at the beginning, formed multilayer structure built of hydrogenated amorphous carbon (a-C:H) (other part of the total coating) (Fig. 5).

It is well known that a-C:H coatings have low friction coefficient and low specific wear rates. Thus, the a-C:H coatings are very promising bio- tribological materials for surgical tools application. However, poor adhesion strength to substrate, high residual stress and weak thermal stability limit the application of a-C:H coatings.[21] In the current work Cr nano- grains have been utilized to modify structure and properties of amorphous carbon. Cr nano- grains were gradually inserted into carbon structure (Fig. 5).

At the STEM image, layered structure of the a- C:H implanted by Cr nano- grains is clearly visible (Fig. 5a). The qualitative chemical analysis EDS (Energy Dispersive X-ray Spectroscopy) has been performed along the line marked at the STEM image (Fig. 5a). The results were presented in the form of the diagram of the selected elements distribution along the line (perpendicular to the substrate) (Fig. 5b). At the Cr line, steps were noticed. They were marked by arrows at the diagram. Each step corresponded to the individual a-C:H layer with different amount of Cr nano- crystals content. The amount of Cr nano- grains was constantly decreasing towards the top of the coating, what has been presented at the maps of selected elements (Fig. 5c). Cr as one of carbide formed elements possesses an attractive combination of properties (corrosion resistance, wear resistance, etc.). Thus, many researchers have paid more attention to the structures and tribological properties of Cr/ a-C:H coatings.[27-31] In case of described coatings, the farther from the interface with

RSC Advances Accepted Manuscript

a Cr/Cr_2N, the degree of a-C:H+Cr nano, the crystallinity was less. It has been well confirmed by selected area electron diffraction patterns (Fig. 6b).

The further the distance from the interface with Cr/Cr_2N part of the total coating, the more amorphous character of diffraction pattern.

3.2. Micromechanical properties of analyzed coatings

The wear rate was calculated for all variants of deposited coatings, but results should be treated only qualitatively due to the fact that the coatings were deposited on carbon- fiber composite substrates. Part of the carbon fibers were not sunk deeply in epoxy and had direct contact with the coating. This resulted in non-standard behavior of coatings subjected to the wear test. Delamination appeared by coating chipping.

Coating which was deposited according to the "D" variant of the deposition condition was not taken under consideration. The residual stress formed during deposition process, caused delamination of the amorphous carbon part of the coating. In the case of the coating deposited in the "A" variant of the deposition conditions the cohesive cracks (first cracks) were formed under 8N. The delamination of the coating (adhesive cracks) was found under 20N of the applied load.

Coating which was deposited in the "B" variant had very low adhesion. The cohesion cracks were formed under 3N, while adhesive ones under 6N. The last coating which was taken under mechanical investigation was deposited according to the "C" variant. The first cracks were formed under 10N, while delamination occurred under 21N.

The second micro- mechanical test was based on micro- indentation using Berkovich indenter. The indenter was loaded up to the formation of first cracks. The cracks formation was indicated by the steps appearance at the diagram (Fig. 7).

The best fracture resistance properties was found for the coating deposited in the "A" variant.

RSC Advances Accepted Manuscript

The next micro- mechanical test was performed to characterize wear resistant properties of analyzed coatings. The test was performed using ball- on- disc mechanical test under 1N and 5N of the uploading (Fig. 8).

Taking under consideration 1N test, for coating deposited under "A" variant of the deposition parameters, the friction coefficient was the lowest. This type of coating was the most wear resistant. From 0 to ~6000 cycle number the friction coefficient raised the fastest, then it had a milder course.

In a first step of the sharper waveform the friction surfaces were adjusted, and some amount of tribo- film was formed. The second stage, where the course was milder, some amount of tribo- film (mainly graphite) occurred. Graphite as a good lubricant could reduce friction.

In case of the coating deposited under "B" variant of the deposition parameters, just at the beginning, the sudden increase, then decrease and again increase of the friction coefficient was observed. This sudden drop of the friction coefficient was also connected with the friction surfaces adjustment. However, it had another character than coating of the "A" variant. Coating deposited under "B" variant had much lower adhesion than deposited in the "A" variant. This sudden jump of the friction coefficient could be connected with the removal of much bigger part of the coating than in the "A" variant. Then there was a stage of the tribo- film formation. The graphite occurrence caused that after some time of the wear process, the friction coefficient courses of the coating deposited under "A" as well as "B" variants were very similar. In case of the coating deposited under "C" variant, friction coefficient was the highest out of analyzed coatings. Its course increased very fast up to 5000 cycles. After this stage the course was stable or even it a little decreased. Probably the formation of high amount of graphite caused this effect.

Looking at the graph of the 5N test the friction coefficient course for coatings deposited under three different deposition parameters were very similar to that which were

RSC Advances Accepted Manuscript

observed in the case of 1N test. In general two stages were visible. The first stage connected with friction surfaces adjustment and the second stage where graphite lubricant reduced the wear. Only the course of the friction coefficient of the coating deposited under "B" variant, did not have this second stage. It may inform that in that case graphite formation did not play significant role in the reduction of the friction coefficient.

3.3. Microstructure characterization of the Cr/Cr_2N + a-C:H+ Cr nano multilayer coating deposited on Carbon Fiber Composite material, after mechanical tests

After the ball- on- disc mechanical test, changes of microstructure caused by mechanical wear were characterized. According to the micro- mechanical test the best properties were found for the coating deposited in the "A" variant. Thus the microstructure changes analysis were done for this type of coating. The topography of coating with wear tracks after 1N and 20000 cycles as well as after 5N and 20000 cycles has been presented at the image done by SEM technique (Fig. 9).

Thin foils for TEM characterization were prepared directly from wear tracks using FIB technique. Only this technique allows to prepare thin foil for TEM and get microstructure information in TEM, precisely from the place of interest (in this case from the wear track).

As a first, changes in microstructure caused by the higher uploading was characterized. 5N test it is too much for such sophisticated, very thin coating, but interesting was the fact how this type of coating was acted under the pressure, of such a large for it, mechanical load.[7]

The cross- section of the coating after 5N test has been presented at the TEM bright field (TEM BF) image. Coating was seriously destroyed and fragmented, however it was still presented at the substrate, fulfilling its protective role (Fig. 10).

Focusing on the upper part of the coating (a-C:H implated by Cr nano- crystals), the role of nano- crystals in amorphous carbon structure has been confirmed (Fig. 11).

RSC Advances Accepted Manuscript

It has been also noticed from diffraction pattern (phase analysis) that Cr nano- crystals inserted into the a-C:H structure, reacted with carbon forming chromium carbide nano- grains ($Cr_{23}C_6$). The HRTEM image presented that crack propagating through a a-C:H layer with lower $Cr_{23}C_6$ nano- particles content has been stopped at the interface with another layer of a-C:H with higher amount of $Cr_{23}C_6$.

The Cr/Cr_2N part of the coating also played an important role in cracking protection process. Cr_2N ceramic layers brittle cracked, while metallic Cr plastically deformed, reducing the cracking energy (Fig. 12 and Fig. 13).

Plastic deformation in metallic Cr layers was realized in 45°, it is a typical angle for plastic deformation of polycrystalline, metallic materials.[24]

During a wear process coating was cracked and fragmented, then parts of the coating were removed in the form of wear debris. In the next step of the wear, the removed material was crushed, mixed together and deposited again at the top of the coating forming so called tribo-film. The tribo- film material is normally formed at the top of material, which is subjected to wear process, as a wear product (Fig. 14).

The phase analysis of the tribo- film, which was performed using selected area electron diffraction technique, indicated presence of chromium nitride (darker spots), and carbon in the form of graphite (bright matrix). The graphite is a very good lubricant.[25] Formation of this material during wear is an advantage, which may reduce friction coefficient.

The 5N and 20000 cycles wear test (ball- on- disc) it was pretty too mach for such type of coating, however as it was proved, even under such high uploading conditions, the coating still fulfilled its role. The suitable uploading for such type of coatings is ~1N. The 1N and 20000 cycles wear test has been performed. After the test, the changes in microstructure have been characterized using transmission electron microscopy technique (Fig. 15).

RSC Advances Accepted Manuscript

Looking at the coating microstructure at the cross- section, it has been found out that coating was not such seriously destroyed as it was after 5N test. No cracks were found. Focusing at the surface topography, it has been noticed that at the top of the coating graphite was formed during the wear process (Fig. 16). The phase analysis done by diffraction pattern, showed presence of graphite and chromium carbides in the tribo- film.

The results were confirmed by high resolution TEM technique (Fig. 17). The graphite material, as a very good lubricant would influence on wear resistant properties of coating during wear process.

3.4. Biological investigations

The cytotoxicity was analyzed using eukaryotic cells (Fig. 18). Variant “A” and “B” of deposition differed only in current conditions, however it influenced on bio- compatible properties of the material. The majority of carbon part of the coating deposited in “A” variant was produced in 230 DC, while the majority of the carbon part of the coating deposited in the “B” variant was produced in 155 DC. It may be concluded that the higher the current of the deposition process the better biological properties. The “C” and “D” was deposited without nitrogen flow. It can be concluded that no nitrogen flow had a negative influence on biological properties of analyzed coatings. In the “D” variant, amorphous carbon was produce only because of the methane flow. There was no graphite target. It resulted in the worst biological properties.

5. Conclusions

RSC Advances Accepted Manuscript

- A hybrid PLD system (Pulsed Laser Deposition + magnetron sputtering) is a suitable technique for a complicated multilayer structure deposition on carbon- fiber- composite materials. This technique is also adequate for coatings deposition on polymers [23]

- Quality of deposited Cr/CrN+a-C:H+ Cr nano multilayer coatings was very high

- Coatings clearly reflects the surface roughness of the carbon- fiber- composite (CFC) substrate

- The same diffraction contrast went through interfaces in Cr/Cr_2N part of the coating, what confirmed crystallographic dependence in between Cr and Cr_2N phases.

- In the current work Cr nano- grains have been utilized to modify structure and properties of amorphous carbon- the second part of the coating; Cr nano- grains were gradually inserted into carbon structure

- After 5N and 20000 cycles wear test (ball-on-disc), coating was seriously destroyed and fragmented, however it was still present at the substrate, fulfilling its protective role

- Cr inserted into amorphous carbon, reacted with carbon forming chromium carbides nano-particles ($Cr_{23}C_6$)

- The HRTEM image presented that crack propagating through a a-C:H layer with lower $Cr_{23}C_6$ nanoparticles content has been stopped at the interface with another layer of a-C:H with higher amount of $Cr_{23}C_6$.

- The Cr/Cr_2N part of the coating also played an important role in cracking protection process. Cr_2N ceramic layers brittle cracked, while metallic Cr plastically deformed, reducing the cracking energy

- 1N and 20000 wear test did not caused serious distraction of the coating. No cracks were found. At the surface of the coating graphite, as a perfect lubricant was formed

- The lowest cytotoxic effect was found for the coating deposited according to the “A” variant of deposition

RSC Advances Accepted Manuscript

- Deposition current and adequate gas flow during coatings production may have an influence on their bio- compatible properties

Acknowledgement to:

- Research Project (National Science Centre): Multilayered, wear resistant, self- healing, protective coatings elaboration for carbon fiber composite materials.
Number: 2012/06/M/ST8/00408

- Research Project (National Science Centre): Bio-mechanical and microstructure analysis of multilayer nano- composite, protective coatings for metallic substrates for tissue interaction. Number: 2012/07/B/ST8/03396

References:

[1]. M.P. Bacos. Journal de Physique IV, 1993, vol. **3**, 1893- 1903

[2]. L. Wieming, D.D.L. Chung. Carbon, 2002, **40**, 1249- 1254

[3]. X. Qiang, H. Li, Y. Zhang, Q. Fu, J. Wei, S. Tian. Corr. Sci., 2011, **53**, 523–527

[4]. G.-Bin Zheng, H. Mizuki, H. Sano, Y. Uchiyama. Carbon, 2008, **46**, 1792– 1828

[5]. Q.-Gang Fu, L. He-Jun, X.-Hong Shi, Ke-Z. Li, J. Wei, M. Huang. Mat. Lett. 2006, **60**, 431–434

[6]. F. Smeacetto, M. Ferraris, M. Salvo. Carbon, 2003, **41**, 2105- 2111

[7] M. Ivosevic, R. Knight, S.R. Kalidindi, G.R. Palmese, J.K. Sutter. J. Therm. Spray Technol., 2005, **14**, 45- 51.

[8] G. Palumbo, I. Brooks, K. Panagiotopoulos. US patent 7387578.

[9] C. Friedrich, R. Gadow, M. Speicher. Surf. Coat. Technol., 2002, **151–152**, 405- 411.

[10] M. Biron. Thermosets and Composites Elsevier, Oxford ISBN: 978-1-4557-7898-0, 2004.

RSC Advances Accepted Manuscript

[11] S. Zhang, D. Sun, Y. Fu, H. Du. Surf. Coat. Technol., 2005, **198**, 2- 8.

[12] A. Karimi, Y. Wang, T. Cselle, M. Morstein. Thin Solid Films, 2002, **420–421**, 275- 280.

[13] Z. Chen, B. Cotterell, W. Wang. Eng. Fract. Mech., 2005, **69**, 597- 603.

[14] T. Kääriäinen, M. Rahamathunnisa, M. Tanttari, D.C. Camer. Proc. of 49th Annual Technical Conference, Washington, DC, USA, April 2006, **22–27**; 548–554.

[15]. J.M. Lackner, L. Major, M. Kot. Bull. Pol. Ac. Sci.: Tech. , 2011, vol.**59**, No. 3, 343-355

[16]. L. Major, J.M. Lackner, B. Major. RSC Adv., 2014, **4**, 21108- 21114

[17]. M. Kot, L. Major, J.M. Lackner. Mat. and Design, 2013, **51**, 280–286

[18]. E. Harry, A. Rouzand, P. Juliet, Y. Paleau. Thin Solid Films, 1999, **342**, 207-213

[19]. Ł.Major, W.Tirry, G Van Tendeloo. Surf. & Coat. Technol., 2008, **202**, 6075-6080

[20]. J. Romero, J. Esteve, A. Lousa. Surf. & Coat. Technol., 2004, **188- 189**, 338- 343

[21]. Q. Wang, F. Zhou, X. Ding, Z. Zhou, C. Wang, W. Zhang, L. K-Y. Li, S.- T. Lee. Tribology Int., 2013, **67**, 104- 115

[22]. J.M. Lackner. Surf. & Coat. Technol., 2005, **200**, 1439- 1444

[23]. R. Major, F. Bruckert, J.M. Lackner, W. Waldhauser, M. Pietrzyk, B. Major. Bull Pol. Ac. Sci.: Tech., 2008, **56**, 223-228

[24]. G. Van Tendeloo, D. Van Dyck, S. J. Pennycook. Handbook of Nanoscopy. Copyright Wiley-VCH; ISBN: 78-3-527-31706-6, 2012

[25]. P. Wiecinski, J. Smolik, H. Garbacz, K.J. Kurzydlowski. Thin Solid Films 2011, **519**, 4069- 4073

[26]. J. Weertman and J. R. Weertman, Elementary Dislocation Theory, Oxford University Press, ISBN 0-19-506900-5, 1992

[27]. W. Dai, P.L. Ke, A.Y. Wang. Vac., 2011, **205**, 792- 797

[28]. V. Singh, J.C. Jiang, E.I. Meletis. Thin Solid Films, 2005, **489**, 150- 158

RSC Advances Accepted Manuscript

[29]. W. Dai, P.L. Ke, A.Y. Wang. Vac., 2011, **85**, 792- 797

[30]. W. Dai, A.Y. Wang. Surf. and Coat. Technol., 2011, **2015**, 2882- 2886

[31]. M. Kot, L. Major, K. Chronowska- Przywara, J.M. Lackner, W. Waldhauser, W. Rakowski. Mat. and Design, 2014, **56**, 981- 989

[32]. W.D. Callister, D.G. Rethwisch. Materials Science and Engineering. Copyright John Wiley & Sons; ISBN: 978-0-470-50586-1, 2011

[33]. S. Okita, A. Matsumur, K. Miura. Thin Solid Films 2003, **443**, 66–70

RSC Advances Accepted Manuscript

Figure captions:

Fig. 1. Microstructure characterization of an as deposited coating; a). image obtained using SEM technique; b). image done by TEM technique in STEM mode

Fig. 2. Microstructure characterization of the coating at the cross- section, done by TEM technique; a). TEM BF image; b). STEM image

Fig. 3. The scheme of the Cr and CrN cell growth assembling[12]

Fig. 4. The HRTEM image of the Cr/Cr_2N interface

Fig. 5. Qualitative EDS chemical analysis; a). STEM image; b). diagram of selected elements distribution along the line marked at the STEM image; c). maps of selected elements

Fig. 6. Microstructure characterization of the amorphous carbon part of the coating (outer part) using TEM technique; a). TEM BF image; b). selected electron diffraction patterns (phase analysis); c). maps of selected elements done by EDS technique

Fig. 7. Results of the indentation test of the coatings performed by Berkovich indenter

Fig. 8. Friction coefficient for the analyzed coatings under 1N and 5N wear test

Fig. 9. Topography image of the coating after 1N and 20000 cycles wear test, and 5N and 200000 wear test, done by SEM technique.

Fig. 10. TEM BF image of the coating after 5N and 20000 wear test

RSC Advances Accepted Manuscript

Fig. 11. Microstructure characterization of the amorphous carbon part of the coating, after 5N and 20000 wear test; a). TEM BF image; b). HRTEM image

Fig. 12. Microstructure characterization of the Cr/Cr_2N part of the coating (first part from the substrate), after 5N and 20000 wear test; a). TEM BF image; b). TEM BF image- higher magnification; c). STEM image

Fig. 13. HRTEM image of the Cr/Cr_2N interface

Fig. 14. Microstructure characterization of the tribo- film, done by TEM technique

Fig. 15. Microstructure characterization of the coating at the cross- section, after 1N and 20000 cycles wear test, done by TEM technique in STEM mode

Fig. 16. Microstructure characterization of the tribo- film formed after 1N and 20000 wear test, done by TEM technique

Fig. 17. The HRTEM analysis of the graphite in the tribo- film formed during the 1N and 20000 cycles wear test

Fig. 18. Cytotoxicity results in dependence on the deposition condition

RSC Advances Accepted Manuscript

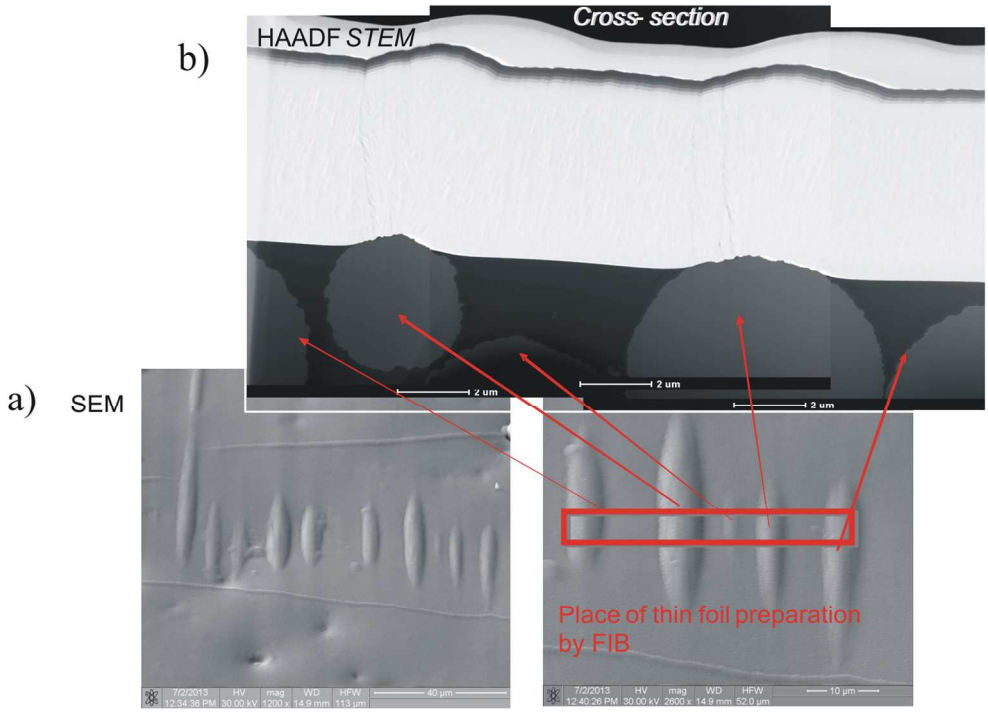

Fig. 1. Microstructure characterization of an as deposited coating; a). image obtained using SEM technique; b). image done by TEM technique in STEM mode
130x91mm (300 x 300 DPI)

RSC Advances Accepted Manuscript

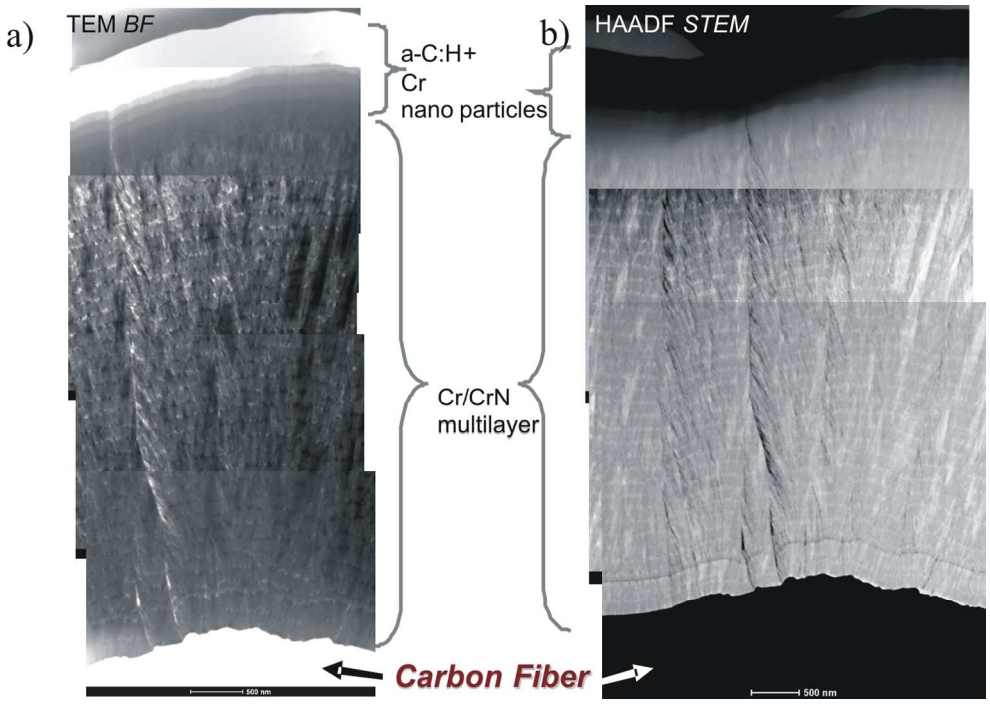

Fig. 2. Microstructure characterization of the coating at the cross- section, done by TEM technique; a). TEM BF image; b). STEM image
136x94mm (300 x 300 DPI)

RSC Advances Accepted Manuscript

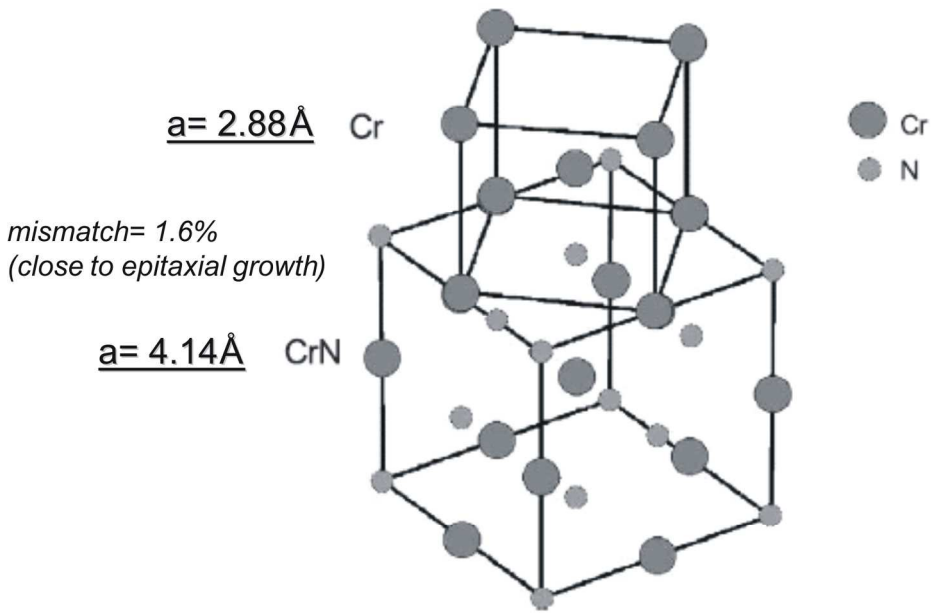

Fig. 3. The scheme of the Cr and CrN cell growth assembling12
175x109mm (300 x 300 DPI)

RSC Advances Accepted Manuscript

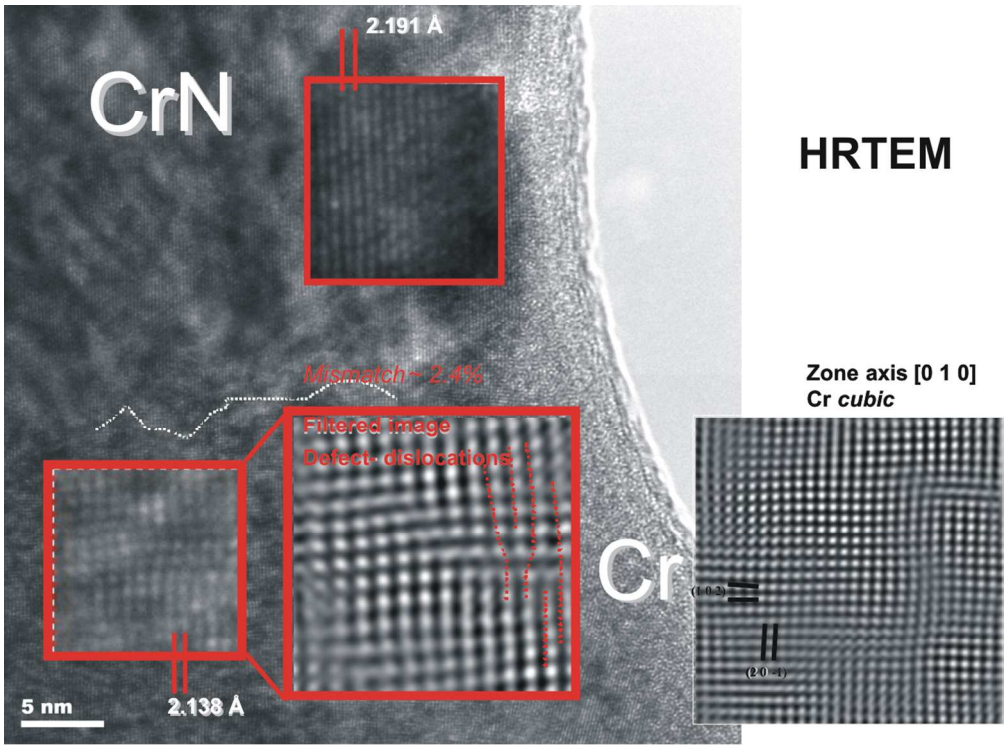

Fig. 4. The HRTEM image of the Cr/Cr2N interface
114x84mm (300 x 300 DPI)

RSC Advances Accepted Manuscript

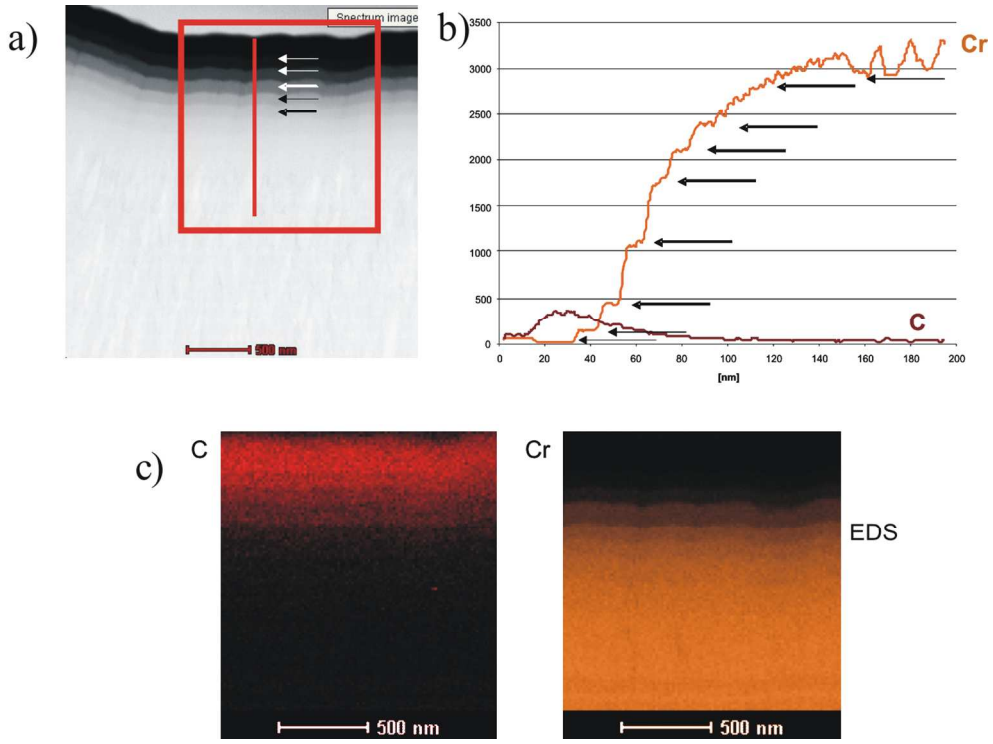

Fig. 5. Qualitative EDS chemical analysis; a). STEM image; b). diagram of selected elements distribution along the line marked at the STEM image; c). maps of selected elements
125x91mm (300 x 300 DPI)

RSC Advances Accepted Manuscript

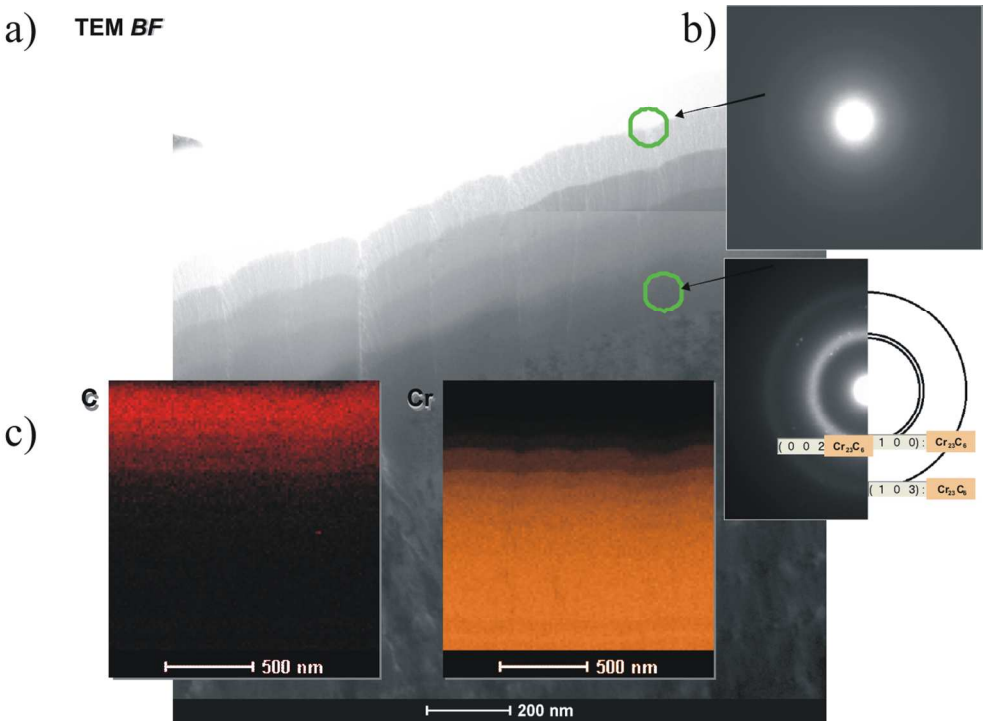

Fig. 6. Microstructure characterization of the amorphous carbon part of the coating (outer part) using TEM technique; a). TEM BF image; b). selected electron diffraction patterns (phase analysis); c). maps of selected elements done by EDS technique
117x83mm (300 x 300 DPI)

RSC Advances Accepted Manuscript

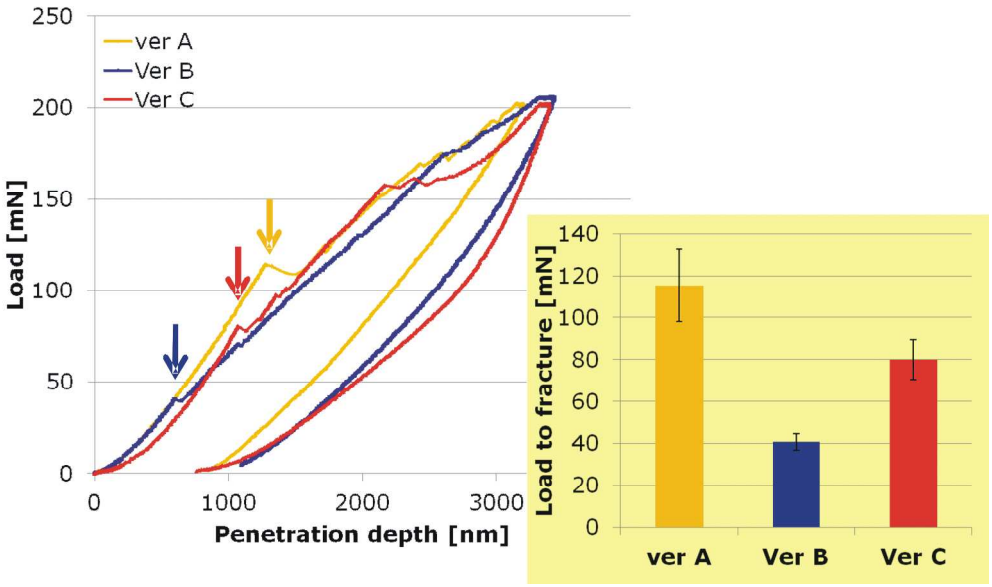

Fig. 7. Results of the indentation test of the coatings performed by Berkovich indenter
254x148mm (300 x 300 DPI)

RSC Advances Accepted Manuscript

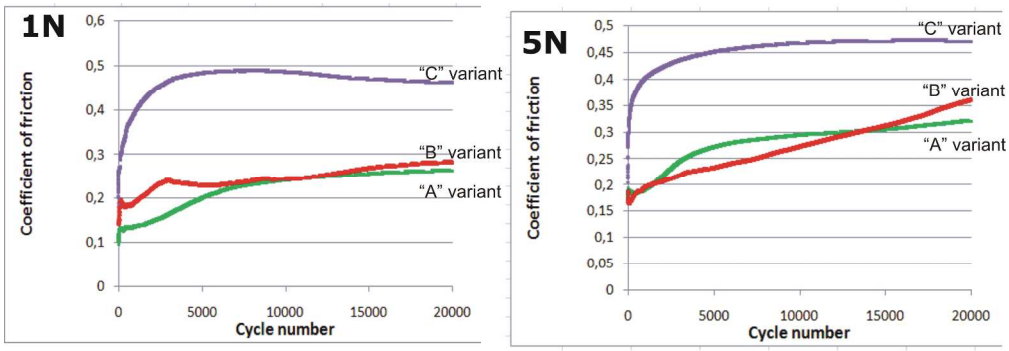

Fig. 8. Friction coefficient for the analyzed coatings under 1N and 5N wear test
277x96mm (300 x 300 DPI)

RSC Advances Accepted Manuscript

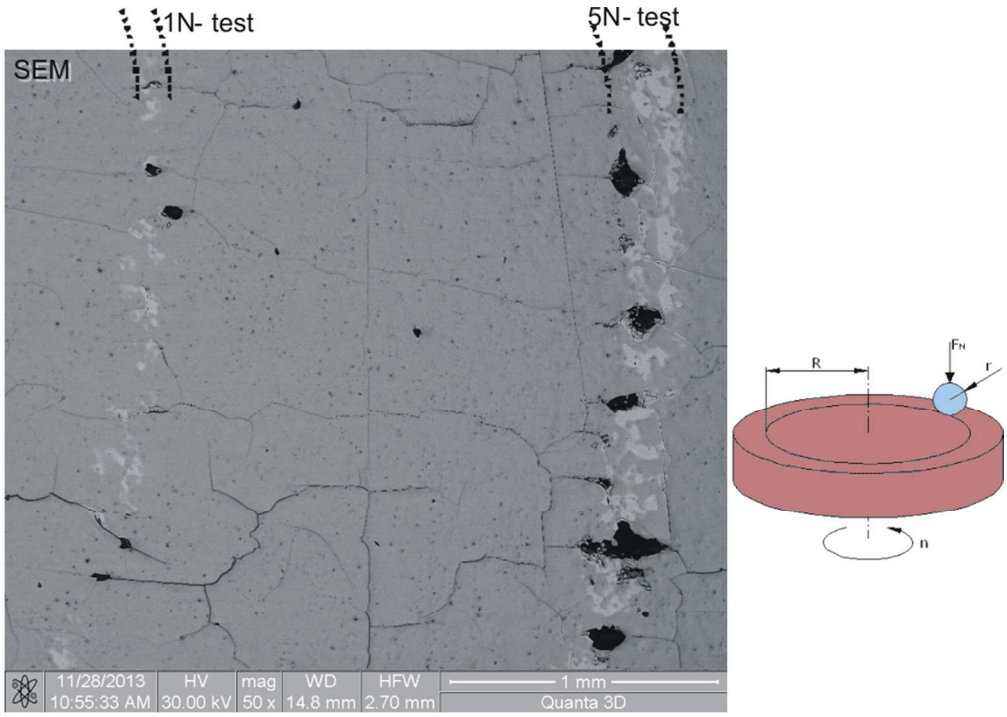

Fig. 9. Topography image of the coating after 1N and 20000 cycles wear test, and 5N and 200000 wear test, done by SEM technique
85x60mm (300 x 300 DPI)

RSC Advances Accepted Manuscript

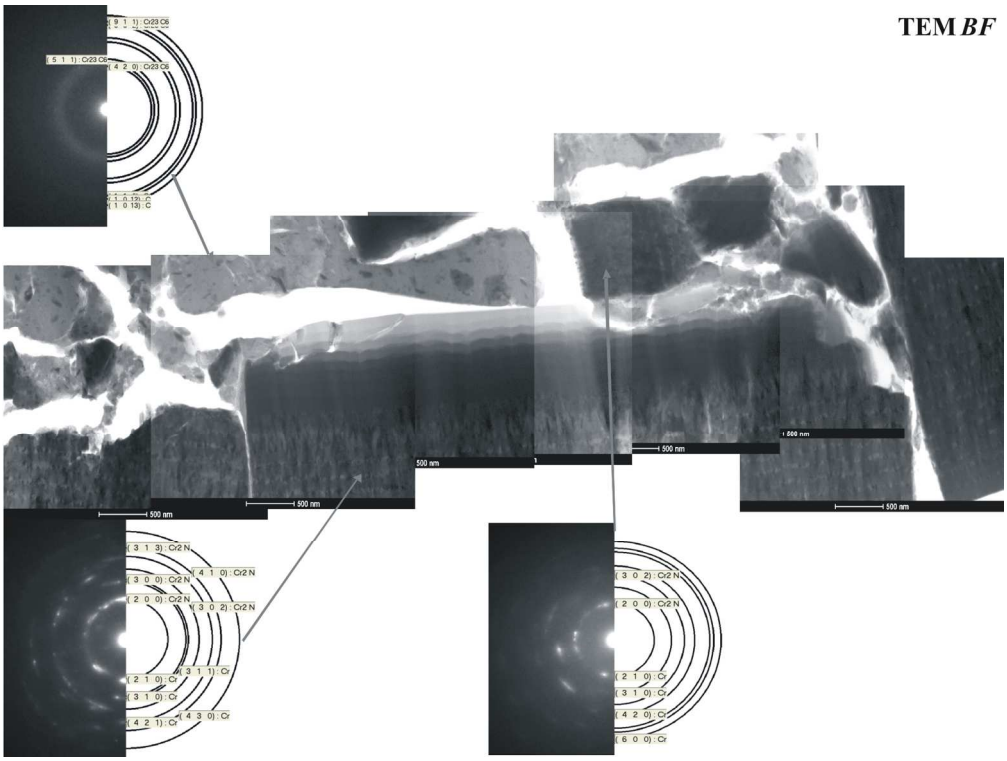

Fig. 10. TEM BF image of the coating after 5N and 20000 wear test
155x116mm (300 x 300 DPI)

RSC Advances Accepted Manuscript

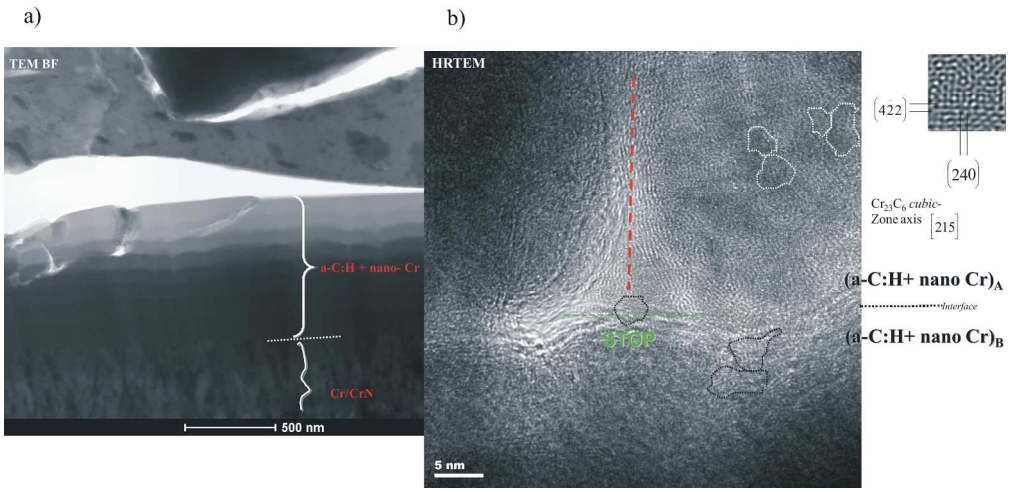

Fig. 11. Microstructure characterization of the amorphous carbon part of the coating, after 5N and 20000 wear test; a). TEM BF image; b). HRTEM image
290x142mm (300 x 300 DPI)

RSC Advances Accepted Manuscript

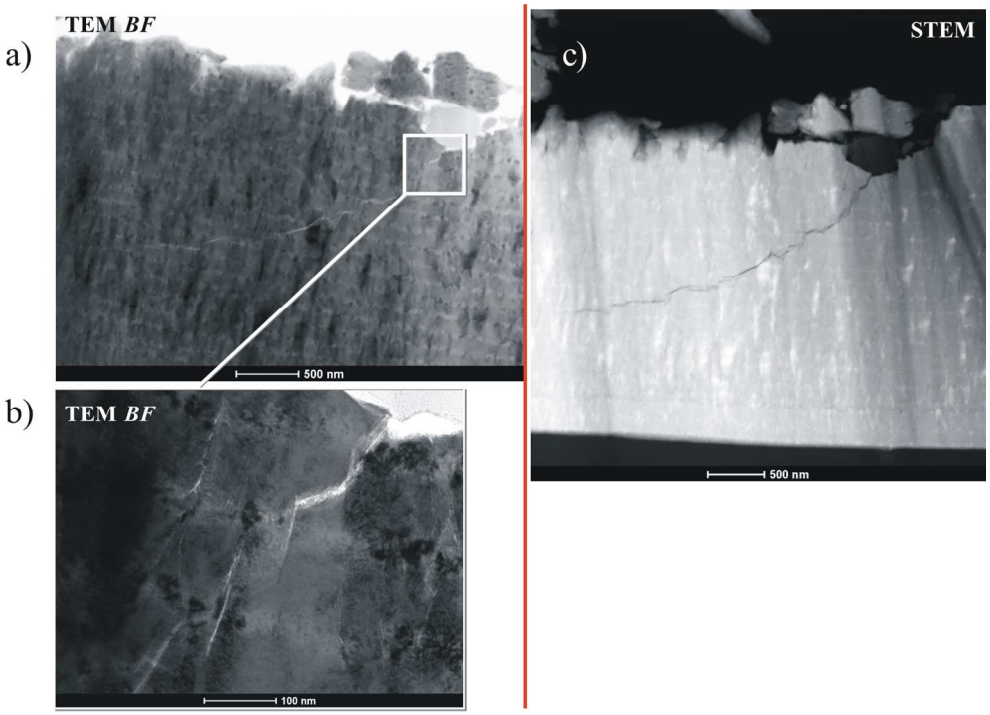

Fig. 12. Microstructure characterization of the Cr/Cr2N part of the coating (first part from the substrate), after 5N and 20000 wear test; a). TEM BF image; b). TEM BF image- higher magnification; c). STEM image

142x100mm (300 x 300 DPI)

RSC Advances Accepted Manuscript

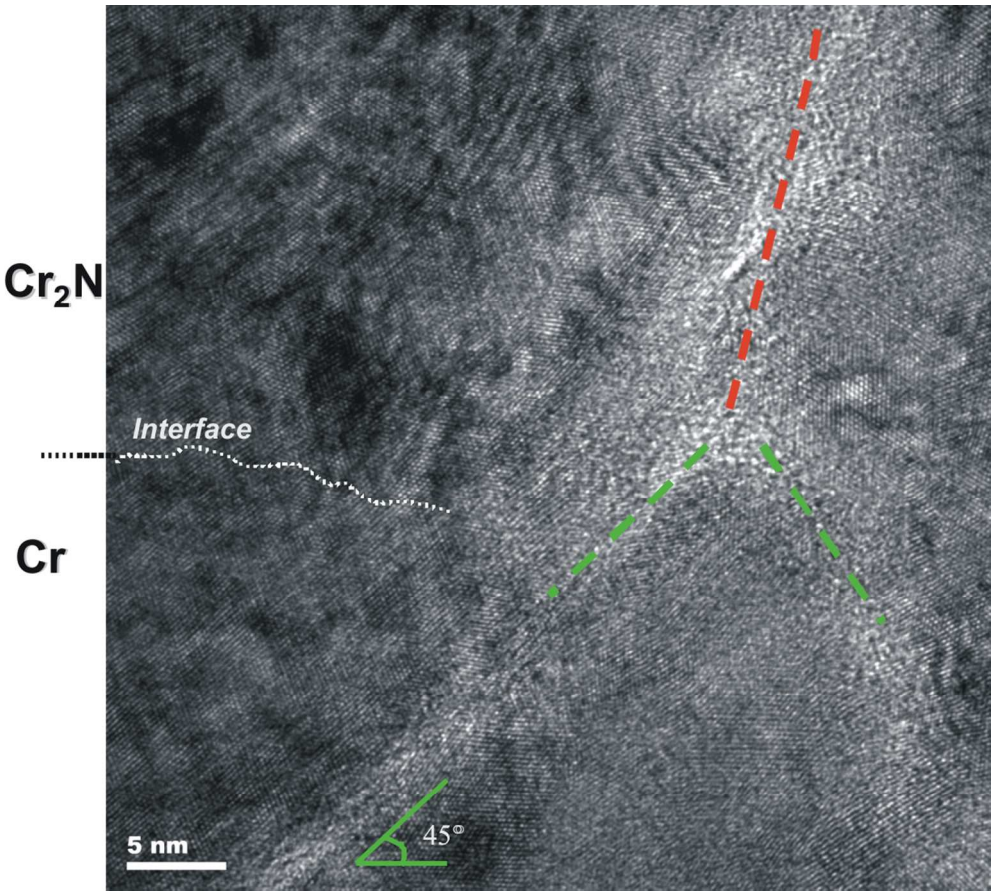

Fig. 13. HRTEM image of the Cr/Cr2N interface
104x92mm (300 x 300 DPI)

RSC Advances Accepted Manuscript

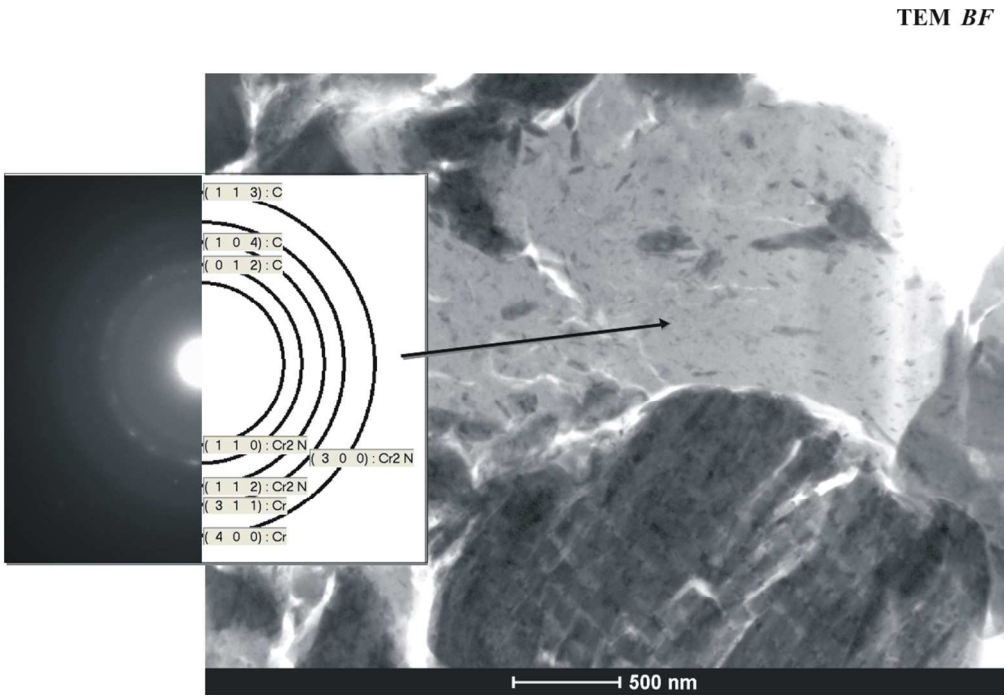

Fig. 14. Microstructure characterization of the tribo- film, done by TEM technique
104x71mm (300 x 300 DPI)

RSC Advances Accepted Manuscript

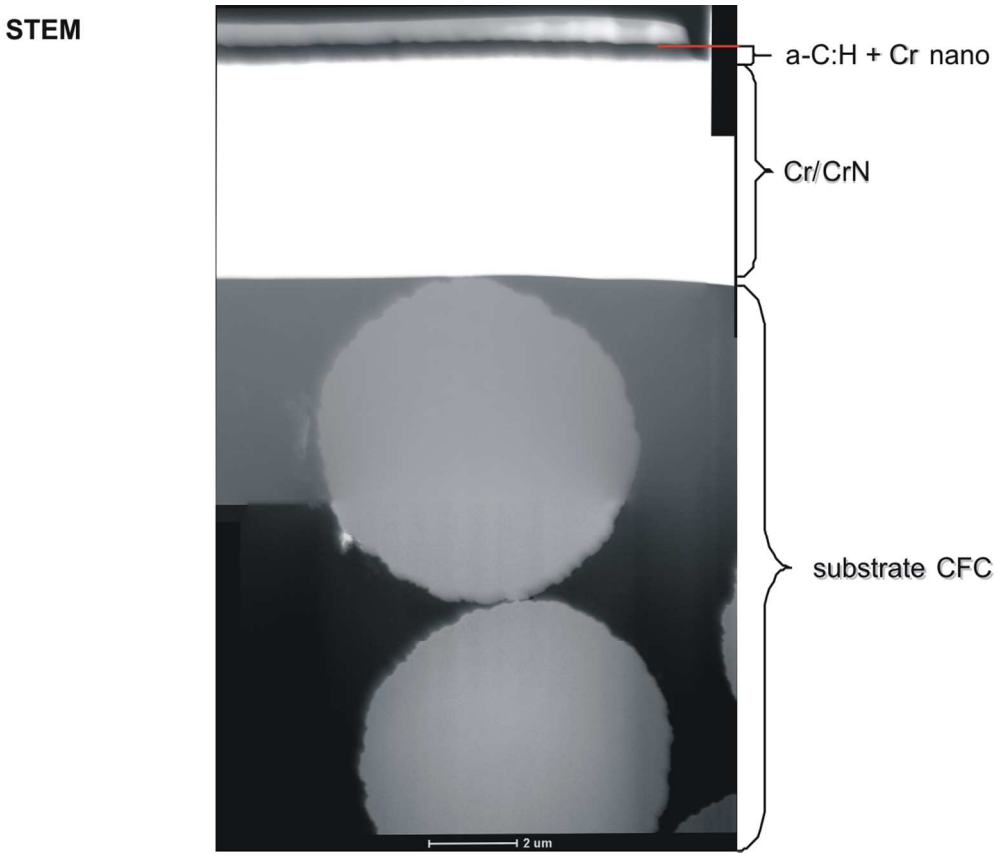

Fig. 15. Microstructure characterization of the coating at the cross- section, after 1N and 20000 cycles wear test, done by TEM technique in STEM mode
109x92mm (300 x 300 DPI)

RSC Advances Accepted Manuscript

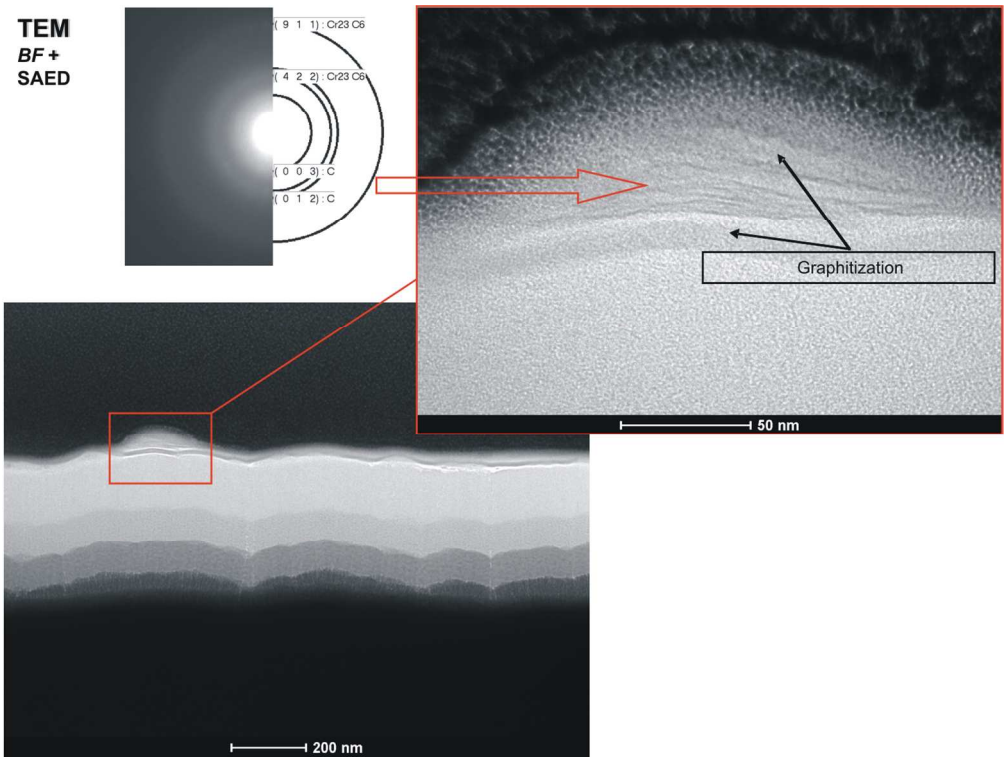

Fig. 16. Microstructure characterization of the tribo- film formed after 1N and 20000 wear test, done by TEM technique
130x97mm (300 x 300 DPI)

RSC Advances Accepted Manuscript

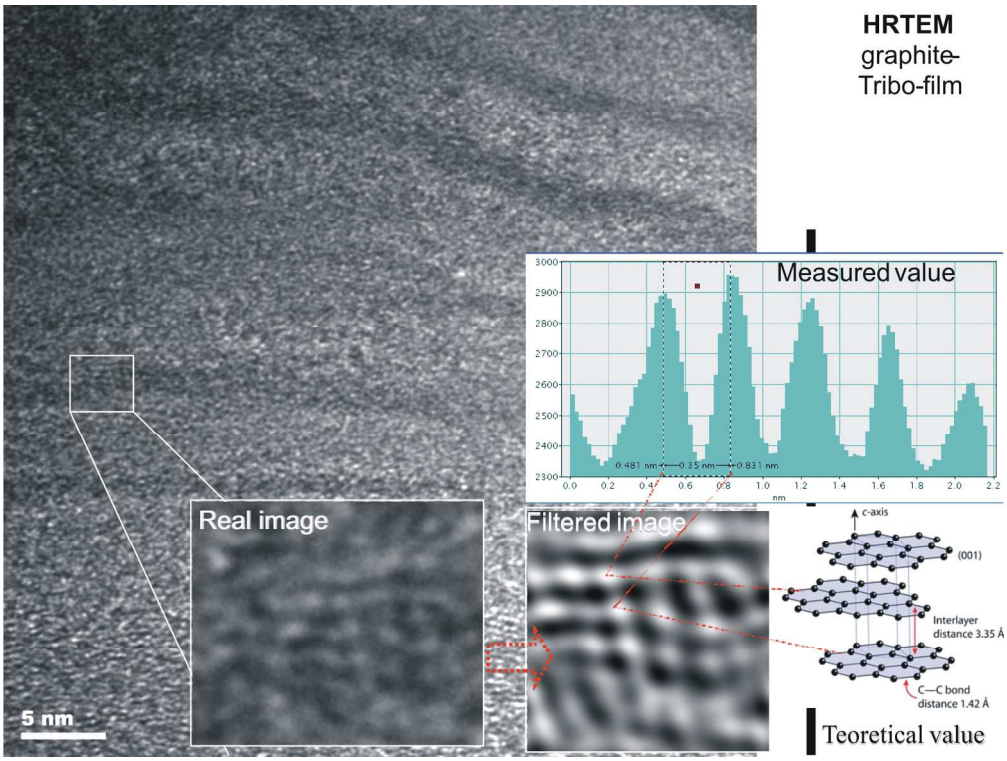

Fig. 17. The HRTEM analysis of the graphite in the tribo- film formed during the 1N and 20000 cycles wear test
165x124mm (300 x 300 DPI)

RSC Advances Accepted Manuscript

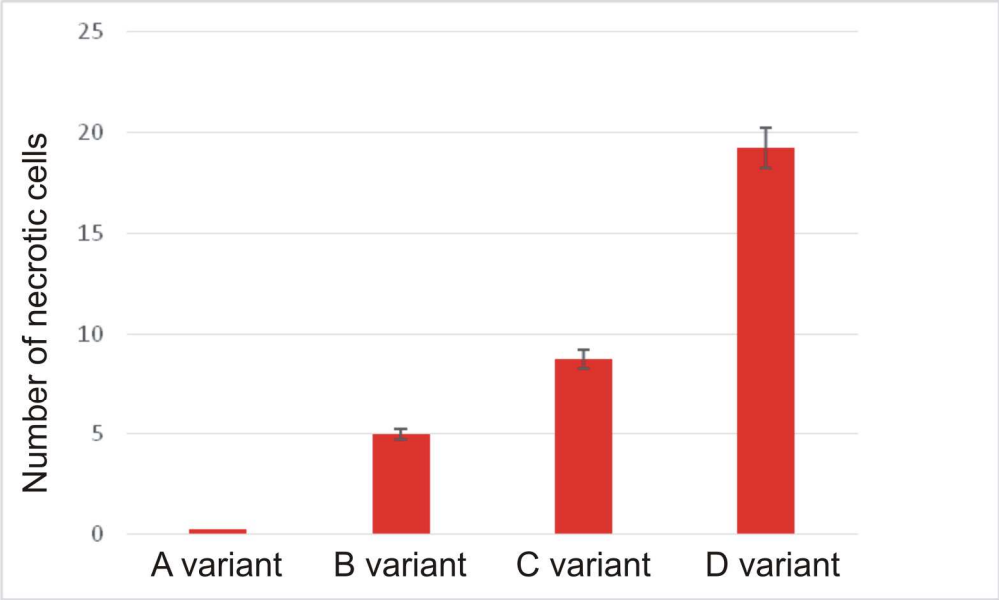

Fig. 18. Cytotoxicity results in dependence on the deposition condition
188x112mm (300 x 300 DPI)

RSC Advances Accepted Manuscript

Table 1. Four different versions (deposition parameters set) of the outer part of the coating deposition

A variant

Step	Cr [W]	C [W]	C_2H_2 [sccm]	Ar [sccm]	N_2 [sccm]	Time [min]	
1	1400	50	5	45	0	14	1/3
2	1230	410	4,5	45,6	0	14	
3	1060	780	3,8	46,2	0	14	
4	890	1150	3,1	45,2	1,7	14	2/3
5	720	1520	2,5	44,2	3,3	14	
6	550	1890	1,9	43,1	5	14	
7	380	2260	1,3	42	6,7	14	
8	210	2630	0,6	41,1	8,3	14	
9	50	3000	0	40	10	14	

B variant

Step	Cr [W]	C [W]	C_2H_2 [sccm]	Ar [sccm]	N_2 [sccm]	Time [min]	
1	1400	50	5	45	0	14	2/3
2	1230	410	4,5	45,6	0	14	
3	1060	780	3,8	46,2	0	14	
4	890	1150	3,1	45,2	1,7	14	
5	720	1520	2,5	44,2	3,3	14	
6	550	1890	1,9	43,1	5	14	
7	380	2260	1,3	42	6,7	14	1/3
8	210	2630	0,6	41,1	8,3	14	
9	50	3000	0	40	10	14	

C variant

Step	Cr [W]	C [W]	C_2H_2 [sccm]	Ar50 [sccm]	N_2 [sccm	Time [min]	
1	1400	50	20	30		14	2/3
2	1230	410	22,5	27,5		14	
3	1060	780	25	25		14	
4	890	1150	27,5	22,5		14	
5	720	1520	30	20		14	
6	550	1890	32,5	17,5		14	
7	380	2260	35	15		14	1/3
8	210	2630	37,5	12,5		14	
9	50	3000	40	10		14	

D variant

Step	Cr [W]	C [W]	C_2H_2 [sccm]	Ar50 [sccm]	N_2 [sccm]	Time [min]	
1	1400		20	30		14	2/3
2	1230		21,9	28,1		14	
3	1060		23,8	26,2		14	
4	890		25,6	24,4		14	
5	720		27,5	22,5		14	
6	550		29,4	20,6		14	
7	380		31,2	18,8		14	1/3
8	210		33,1	16,9		14	
9	50		35	15		14	

RSC Advances Accepted Manuscript